identity. Thus, the presence of cmnm^{5}U in mitochondrial tRNAs reading two-codon families ending in a purine seems to be an evolutionarily conserved mechanism to prevent misreading of pyrimidine as the third position of codon.

ACKNOWLEDGMENTS

We thank Dr. H. Ishikura for the gift of an authentic sample of cmnm^{5}U, Dr. S. Yokoyama for helpful discussion, and S. C. Pomerantz for technical assistance.

REFERENCES

Björk, G. (1984) in *Processing of RNA* (Apirion, D., Ed.) pp 291–330, CRC Press, Boca Raton, FL.

Buck, M., Connick, M., & Ames, B. (1983) *Anal. Biochem. 129*, 1–13.

Dirheimer, G. (1983) *Recent Results Cancer Res. 84*, 1–46.

Dirheimer, G., & Martin, R. P. (1990) in *Chromatography and Modification of Nucleosides, Vol. II: Biochemical Roles and Function of Modification* (Gehrke, C. W., & Kuo, K. C., Eds.) Elsevier Chromatography Library Series, Elsevier, Amsterdam (in press).

Edmonds, C. G., Vestal, M. L., & McCloskey, J. A. (1985) *Nucleic Acids Res. 13*, 8197–8206.

Gehrke, C. W., & Kuo, K. C. (1989) *J. Chromatogr. 471*, 3–36.

Gehrke, C. W., & Kuo, K. C. (1990) in *Chromatography and Modification of Nucleosides, Vol. I: Analytical Methods for Major and Modified Nucleosides* and *Oligonucleotides* (Gehrke, C. W., & Kuo, K. C., Eds.) Elsevier Chromatography Library Series, Elsevier, Amsterdam (in press).

Gehrke, C. W., Kuo, K. C., McCune, R. A., Gerhardt, K. O., & Agris, P. F. (1982) *J. Chromatogr. Biomed. Appl. 230*, 297–308.

Hagervall, T. G., Edmonds, C. G., McCloskey, J. A., & Björk, G. R. (1987) *J. Biol. Chem. 262*, 8488–8495.

Heckman, J. E., Sarnoff, J., Alzner-DeWeerd, B., Yin, S., & RajBhandary, U. L. (1980) *Proc. Natl. Acad. Sci. U.S.A. 77*, 3159–3163.

Hillen, W., Egert, E., Lindner, H. J., & Gassen, H. G. (1978) *FEBS Lett. 94*, 361–364.

Martin, R. P., Schneller, J. M., Stahl, A. J. C., & Dirheimer, G. (1977) *Nucleic Acids Res. 4*, 3497–3510.

Martin, R. P., Sibler, A.-P., Bordonnê, R., & Dirheimer, G. (1983) *Mol. Biol. (Moscow) 17*, 1126–1146.

Michelson, A. M. (1963) *The Chemistry of Nucleosides and Nucleotides*, Academic Press, London.

Miyazawa, T., & Yokoyama, S. (1985) *Proc. Int. Biomol. Struct. Interact. Suppl. J. Biosci. 8*, 731–737.

Murao, K., & Ishikura, H. (1978) *Nucleic Acids Res. 5*, s333–s336.

Phillipson, D. W., Edmonds, C. G., Crain, P. F., Smith, D. L., Davis, D. R., & McCloskey, J. A. (1987) *J. Biol. Chem. 262*, 3462–3471.

Sibler, A.-P., Bordonnê, R., Dirheimer, G., & Martin, R. P. (1980) *C. R. Acad. Sci. Paris 290*, 695–698.

Sibler, A.-P., Dirheimer, G., & Martin, R. P. (1986) *FEBS Lett. 194*, 131–138.

Randerath, E., Agrawal, H. P., & Randerath, K. (1981) *Biochem. Biophys. Res. Commun. 103*, 739–744.

Yokoyama, S., Watanabe, T., Murao, K., Ishikura, H., Yamaizumi, Z., Nishimura, S., & Miyazawa, T. (1985) *Proc. Natl. Acad. Sci. U.S.A. 82*, 4905–4909.

Yokoyama, S., Muramatsu, T., Kawai, G., Horie, N., Yamaizumi, Z., Kuchino, Y., Nishimura, S., Sekine, M., Hata, T., Matsuda, A., Ueda, T., Goldman, E., & Miyazawa, T. (1987) *11th Int. tRNA Workshop, Umea*, Abstract IIIa-4.

Reduced DNA Flexibility in Complexes with a Type II DNA Binding Protein†

Torleif Härd*,‡ and David R. Kearns

Department of Chemistry, University of California at San Diego, La Jolla, California 92093-0342

Received June 1, 1989; Revised Manuscript Received August 24, 1989

ABSTRACT: We studied internal molecular motions in *Bacillus subtilis* phage SPO1 DNA using the time-resolved fluorescence polarization anisotropy (FPA) of intercalated ethidium. The torsional flexibility of this (hydroxymethyl)uracil-containing DNA is very similar to that of naturally occurring thymine-containing DNAs, as judged from fits of the time-resolved FPA decay to an elastic DNA model. Binding of transcription factor 1 (TF1), a type II procaryotic DNA binding protein encoded by the phage SPO1, enhances the FPA, indicating a substantial decrease in the average DNA torsional flexibility in the DNA–TF1 complex. The FPA increase is correlated with a reduced ethidium binding affinity. The effects can be noticed at TF1 binding ratios less than 1 TF1 dimer/500 DNA base pairs, and the measured torsional rigidity at high TF1 binding ratios (1 TF1 dimer/15–20 DNA base pairs) is about 7 times greater than in the absence of TF1. On the basis of a discussion of various mechanisms for the observed effect we argue that it is due to protein-induced DNA bending at low binding densities although other explanations are also possible. This interpretation might have implications for understanding the biological function of TF1.

The type II DNA binding proteins (DBPII)[1] are a family of small (monomer MW ≈ 10000) basic procaryotic proteins (Drlica & Rouviere-Yaniv, 1987) that have a high degree of sequence homology. DBPII have been shown to induce DNA bending and compaction, and it has been inferred that this might be one of the mechanisms by which they function biologically. For instance, the DBPII from *Escherichia coli* (the HU protein) share some common properties with eukaryotic

† This work was supported by grants from the NSF (DMB8604545) and the NIH (PHS GM40635) (to D.R.K.) and by a postdoctoral fellowship from the Swedish Natural Sciences Research Council (to T.H.).

‡ Present address: Department of Medical Biophysics, Karolinska Institute, Box 60400, S-10401 Stockholm, Sweden.

[1] Abbreviations: DBPII, type II DNA binding proteins; IHF, integration host factor; TF1, transcription factor 1; hmUra, (hydroxymethyl)uracil; FPA, fluorescence polarization anisotropy; bp, base pair; ARF, amplitude reduction factor; EDTA, ethylenediaminetetraacetic acid.

0006-2960/90/0429-959$02.50/0

histones, e.g., the ability to induce DNA compaction and to restrain negative supercoils [Drlica & Rouviere-Yaniv (1987) and references cited therein]. The structure of the HU from *Bacillus stearothermophilus* has been solved by X-ray crystallography, and a model of the HU–DNA complex in which two extended "loops" of the HU dimer bind the DNA was proposed on the basis of this structure. It was also suggested how bound HU dimers might interact to bend the DNA (Tanaka et al., 1984). Another DBPII, the *E. coli* integration host factor (IHF), affects gene expression and DNA replication by binding to specific sequences in the genome (Drlica & Rouviere-Yaniv, 1987). It has been demonstrated that IHF induces DNA bending at specific sites, in analogy with the proposed action of the HU protein (Stenzel et al., 1987; Robertson & Nash, 1988).

The transcription factor 1 (TF1) is the DBPII encoded by the *Bacillus subtilis* phage SPO1, whose DNA contains (hydroxymethyl)uracil (hmUra) instead of thymine (Wilson & Geiduschek, 1969; Johnson & Geiduschek, 1972; Greene et al., 1984). At low binding ratios, TF1 occupies a limited number of specific sites on the SPO1 genome. These sites are hmUra-specific as well as sequence-specific, and they involve occupancy of a core site at low TF1 concentrations, with binding to adjacent DNA as the protein concentration increases (Greene & Geiduschek, 1985a,b). There is no common consensus sequence for the strongest binding sites, and it has been suggested that the local DNA conformation and/or susceptibility to bending might determine the sequence-specific binding, so that the initial TF1 complex, and adjacently bound TF1 proteins, might induce DNA bending and supercoiling (Greene & Geiduschek, 1985b).

In this study we use time-resolved and steady-state fluorescence polarization anisotropy (FPA) of intercalated ethidium to examine the torsional flexibility in hmUra-containing SPO1 DNA and changes in the apparent flexibility induced by TF1 binding. The FPA of intercalated dyes is a sensitive measure of DNA motions on a nanosecond timescale (Wahl et al., 1970; Millar et al., 1982; Thomas & Schurr, 1983; Härd et al., 1989a). The time-resolved FPA decay can be fitted to an elastic model of DNA with the DNA torsional rigidity (α) as the only adjustable parameter (Allison & Schurr, 1979; Barkley & Zimm, 1979; Schurr, 1984). The "wavelength" of the predominant mode of torsional DNA motions, occurring on the nanosecond timescale, is in the order of $\approx$100 base pairs (Millar et al., 1982). The FPA is therefore very sensitive to changes in the DNA conformation that would interrupt these long-range cooperative motions, and this has been demonstrated for DNA in nucleosomes (Schurr & Schurr, 1985) and chromatin fibers (Ashikawa et al., 1983; Härd et al., 1988), and for the effect of covalently bound *cis*-diamminedichloroplatinum(II) (Millar et al., 1988). Similarly, we would expect DNA bending in TF1–SPO1 DNA complexes to result in an apparent increase in the measured DNA torsional rigidity. On the other hand, if TF1 binding does not affect the FPA of intercalated ethidium, then this could be taken as strong evidence that TF1 does not induce DNA bending.

Materials and Methods

Materials. TF1 protein and phage SPO1 DNA, purified according to previously published procedures (Härd et al., 1989b), were kindly provided by M. H. Sayre at the Center for Molecular Biology at UCSD. Stock solutions of DNA and TF1 were dialyzed against the experimental buffer (50 mM NaCl, 10 mM Tris-HCl, and 2 mM Na_2EDTA at pH 7) and kept frozen (−20 °C) when not in use. The high molecular weight SPO1 DNA (145 kbp) was pipetted carefully to minimize shearing. Ethidium bromide was obtained from Sigma Chemical Co. and dissolved in buffer without further purification. DNA–dye samples were prepared by adding DNA stock solutions to a prediluted ethidium solution. Dye/DNA base pair ratios were kept low (<0.01) to avoid effects of energy transfer or other artifacts on the measured FPA. Titrations of DNA–dye samples with TF1 were carried out by first dividing a DNA–dye sample in two equal volumes and then adding TF1 stock solution to one of the samples and an equal volume of buffer to the other. The TF1-containing solution was then titrated on the non-TF1 solution. DNA and ethidium concentrations were, in this way, kept constant during the titrations. All experiments were carried out at room temperature (22–23 °C).

Fluorescence Measurements and Data Analysis. Steady-state fluorescence was measured on an Aminco SPF-500 spectrofluorometer with Polaroid sheet polarizers in the excitation and emission paths. The steady-state FPA, denoted $\langle r \rangle$, was calculated from

$$\langle r \rangle = \frac{I_{VV} - GI_{VH}}{I_{VV} + 2GI_{VH}} \quad (1)$$

where the subscripts refer to vertical and horizontal positionings of the excitation and emission polarizers, respectively, and $G = I_{HV}/I_{HH}$ corrects for polarizing effects in the emission monochromator and detector. The denominator in eq 1 is proportional to the fluorescence intensity.

Time-resolved fluorescence intensity decays were measured in the laboratory and Prof. Doug Magde at UCSD, using a time-correlated photon-counting instrument that has recently been described elsewhere (Skibsted et al., 1987). For ethidium excitation we used the 514.5-nm line of an actively mode-locked Spectra Physics Ar^+ laser. The excitation light was passed through a Coherent cavity dumper to obtain a convenient pulse repetition rate ($\approx$2.5 MHz). The polarized components of the ethidium fluorescence decay were selected by using a Polaroid sheet polarizer oriented parallel or perpendicular to the polarization of the excitation beam. The emission was then passed through a Specs monochromator set at 600 nm (5-nm band-pass), and time-resolved decays were collected on a multichannel analyzer (1024 channels with 80 ps/channel) and transferred to a computer (Sun-3) for further analysis. The instrument response function to be used in the deconvolution (full width at half-maximum $\approx$750 ps) was recorded from the Raman scattering (at 625 nm) of a sample of pure water (no emission polarizer). Residual background light scattering was collected from blank DNA and DNA/protein samples and subtracted from the ethidium fluorescence decays before fitting the data. The steady-state FPA of the samples (measured on the Aminco) was used to correct for polarizing effects in the monochromator and photomultiplier tube. This was done by calculating the total number of counts for the two polarized components and calculating the correction factor G as

$$G = \frac{\sum_i I_{\parallel}(i)}{\sum_i I_{\perp}(i)} \frac{1 - \langle r \rangle}{1 + 2\langle r \rangle} \quad (2)$$

where $I_{\parallel}(i)$ and $I_{\perp}(i)$ denote the number of counts in channel i for the parallel and perpendicular polarizations (corresponding to I_{VV} and I_{VH} in eq 1) and $\langle r \rangle$ is the measured (and corrected steady-state FPA. The truncation errors in the integration were estimated to result in a total error of <1% in G (for the sample with the longest average fluorescence

lifetime). The observed time-resolved intensity and FPA decays [$I_{obs}(t)$ and $r_{obs}(t)$] were calculated in analogy with eq 1.

The best-fit intensity decay $I(t)$ was deconvoluted from the observed decay and the instrument response function $e(t)$ according to

$$I_{obs}(t) = \int_0^t e(t-t')\, I(t')\, dt' \quad (3)$$

and a nonlinear least-squares fitting program based on the Marquardt algorithm (Press et al., 1986). The best-fit theoretical expression for $I(t)$ was then used to deconvolute and fit an expression for the theoretical FPA decay $r(t)$ according to

$$r_{obs}(t) = \frac{\int_0^t e(t-t')\, r(t')\, I(t')\, dt'}{\int_0^t e(t-t')\, I(t')\, dt'} \quad (4)$$

The fits were judged from reduced χ_r^2 values and plots of weighted residuals (O'Connor & Phillips, 1984). All estimated standard deviations were calculated as described by Wahl (1979).

Fluorescence Polarization of DNA Complexes. A general expression for the FPA, $r(t)$, of a chromophore bound to a deformable macromolecule with a mean local cylindrical symmetry (DNA) has been given by Schurr (1984):

$$r(t) = \mathrm{ARF} \sum_{n=0}^{2} \beta_n\, G_n(t)\, F_n(t) \quad (5)$$

where ARF is an (experimentally determined) amplitude reduction factor due to rapid restricted dye wobbling (Magde et al., 1983; Schurr, 1984; Shibata et al., 1985), the β_n factors depend on the binding site geometry (eq 8), and the correlation functions $G_n(t)$ and $F_n(t)$ reflect molecular motions about the DNA long axis and an axis perpendicular to the DNA long axis, respectively. Analytical expressions for the "torsion" correlation function, $G_n(t)$, of an elastic filament have been derived by Barkley and Zimm (1979) and by Allison and Schurr (1979). Previous experiments with ethidium bound to high molecular weight DNAs have shown that the intermediate zone approximation

$$G_n(t) = \exp(-n^2 C \sqrt{t}) \quad (6)$$

accurately describes the FPA decay at times longer than ≈1 ns, where rapid uncorrelated motions can be neglected, and at times shorter than 70–120 ns, where end effects can be neglected (Thomas et al., 1980; Shibata et al., 1985). The constant C is related to the torsional rigidity constant α as

$$C = k_B T / \sqrt{\pi \alpha \gamma} \quad (7)$$

where k_B is the Boltzmann constant, T is the temperature, and γ is the friction factor for rotation of a base pair [$\gamma = 6.4 \times 10^{-23}$ erg s (Wu et al., 1987)]. In this analysis we assume that $F_n(t) = 1$ for $t < 60$ ns, because the effect of DNA bending motions on a nanosecond time scale can be neglected (Elias & Eden, 1981; Hagerman, 1981; Shibata et al., 1985).

The β_n factors in eq 5, which depend on the angle between the absorption and emission transition moment (for the $S_1 \leftarrow S_0$ transition in ethidium) and the helix axis (θ), are given by

$$\beta_0 = 0.1(3\cos^2\theta - 1)^2 \quad (8a)$$

$$\beta_1 = 0.3(\sin 2\theta)^2 \quad (8b)$$

$$\beta_2 = 0.3 \sin^4\theta \quad (8c)$$

The ethidium binding site geometry has been estimated to $\theta = 71°$ from linear dichroism (LD) measurements of oriented DNA samples (Hogan et al., 1979). Due to some uncertainty in this determination we caution against overinterpretation of the absolute value of α when this parameter is obtained from fits of eq 6 and 7. On the other hand, relative changes in α are still relevant, provided that the ethidium binding site geometry has not changed.

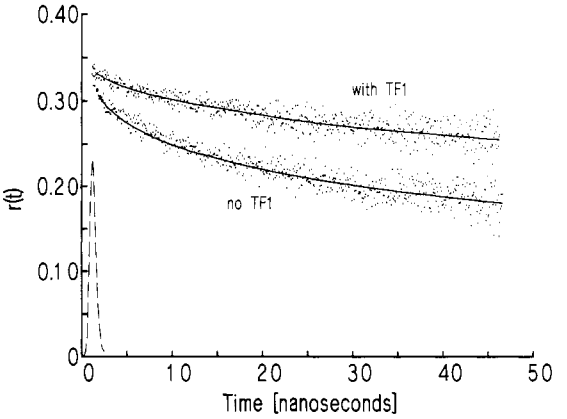

FIGURE 1: Time-resolved FPA decays of ethidium bound to SPO1 DNA in the absence and presence of TF1 [50 μM (bp) DNA, 0.5 μM ethidium, and no TF1 or 5 μM TF1 dimers in 50 mM NaCl, 10 mM Tris-HCl, and 2 mM Na_2EDTA at pH 7]. Solid lines represent fits to eq 5 and 6 (best-fit parameters are given in Table I) and the dashed line is the instrument response function (lamp pulse).

Table I: Fluorescence Intensity and FPA Decay Parameters for Ethidium–SPO1 DNA Samples[a]

sample	Intensity lifetime (ns)	amplitude (%)	χ_r^2
no TF1	2.6 ± 2.0	8 ± 4	1.86
	22.6 ± 0.2	92 ± 4	
with TF1[b]	2.3 ± 0.3	11 ± 1	1.65
	22.4 ± 0.1	89 ± 1	

sample	FPA ARF	C ($ns^{-1/2}$)	α (erg × 10^{12})[c]	χ_r^2
no TF1	0.85 ± 0.01	0.049 ± 0.002	3.5 ± 0.3	1.84
with TF1[b]	0.86 ± 0.01	0.0178 ± 0.002	27 ± 1	1.62

[a] 50 μM (bp) SPO1 DNA and 0.5 μM ethidium in 50 mM NaCl, 10 mM Tris-HCl, and 2 mM Na_2EDTA at pH 7. [b] As above with 5.0 μM (dimers) TF1. [c] Calculated from eq 7 by assuming that $\gamma = 6.4 \times 10^{-23}$ erg s (Wu et al., 1987).

Results

The time-resolved FPA decays of ethidium bound to SPO1 DNA with and without TF1 are shown in Figure 1 and the best-fit parameters for the corresponding fluorescence intensity and FPA decays are listed in Table I. The fluorescence intensity decays are double exponential due to emission from free and bound ethidium. The fluorescence lifetime of bound ethidium is 22.5 ns, in agreement with other fluorescence studies of DNA–ethidium complexes (Thomas et al., 1980; Millar et al., 1982; Thomas & Schurr, 1983). The fluorescence lifetime of free ethidium is not determined with great accuracy (in these experiments) because it is short (≈2 ns), and because the total fraction of the emission due to this component is small (≈1%). The amplitude of the free dye emission is somewhat larger in the TF1-containing sample, indicating that some dye is displaced upon TF1 binding. This effect is demonstrated more clearly in the steady-state fluorescence titrations described below. A fit of the time-resolved FPA to eq 5 and 6 yields a torsional rigidity constant $\alpha = 3.5 \times 10^{-12}$ erg. This value is identical with those previously obtained with calf thymus DNA (Millar et al., 1982) and phage φ29 DNA (Thomas & Schurr, 1983) (3.5×10^{-12} and 3.6×10^{-12} erg, respectively) when the same model and

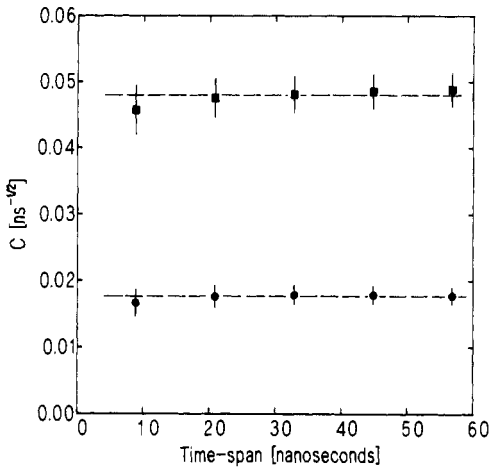

FIGURE 2: Fitted value of the torsional parameter C (eq 6 and 7), as a function of the time span of the FPA decay (measured from the excitation pulse maximum) that is used in the fit. Squares and circles represent fits to FPA decays of ethidium bound to SPO1 DNA in the absence and presence of bound TF1, respectively. Error bars are estimated standard deviations.

ethidium binding site geometry is assumed. The measured torsional rigidity is also independent of the fitted time span (0–8 to 0–58 ns) as shown in Figure 2, and this indicates that the DNA flexibility is uniform over a range of several hundred base pairs (Allison & Schurr, 1979; Thomas & Schurr, 1983), i.e., there are no frequently occuring flexible "joints" in the SPO1 DNA.

However, the time-resolved FPA is dramatically affected by TF1 binding (Figure 1). A fit of the FPA decay for the TF1–SPO1 complex (at a binding density of ≈1 TF1 dimer/15–20 DNA bp) yields a torsional regidity that is about 7 times larger ($\alpha = 27 \times 10^{-12}$ erg, assuming that γ is constant) than in free SPO1 DNA. The fit is good, as judged from $\chi_r^2 = 1.6$ and a plot of the weighted residuals (not shown), indicating that the "intermediate zone approximation" of the elastic DNA model still provides an accurate description of the FPA decay. [This notion is also supported by the fact that the measured torsional rigidity is independent of the fitted time span (Figure 2).] Note, however that the reduced flexibility is not necessarily caused by a larger α but that it might also result from larger "effective" friction factor (γ), or a combination of these effects (see eq 7). It may also be argued that the larger fraction of free ethidium in the TF1-containing sample might influence the fit, but the effect of low concentrations of free dye is expected to be small (it can be neglected at $t > 5$ ns) (Millar et al., 1982). It should also be noted that the neglect of a larger fraction of free dye results in an underestimate rather than an overestimate of the torsional rigidity. The observed decrease in the measured DNA flexibility in TF1–SPO1 DNA complexes might be caused by several mechanisms, and these are discussed below.

Panels A and B of Figure 3 show the effect of increasing TF1 concentrations on the steady-state ethidium FPA and fluorescence intensity, respectively, in a sample containing 22 μM (bp) SPO1 DNA. The results are presented both as plots against the total TF1 dimer concentration (inserts) and verus the binding density ν. The binding density was estimated on the basis of a previously described titration, performed at the same DNA and buffer conditions, where the quenching of TF1 (Tyr94) fluorescence was used as an indicator of the fraction of bound TF1 (Härd et al., 1989b). It is evident that the ethidium FPA and fluorescence intensity is affected at very low TF1 binding densitites (<1 TF1 dimer/500 DNA bp). The FPA increases approximately linearly with the binding

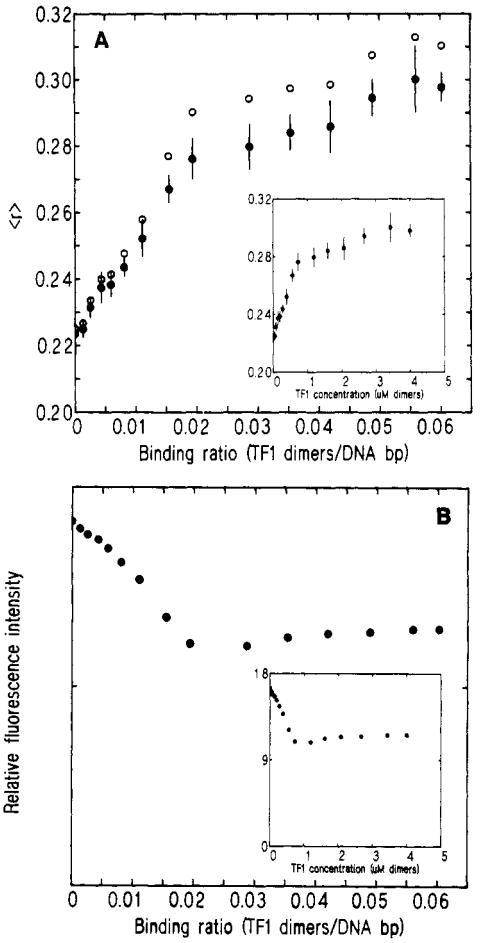

FIGURE 3: (A) Effect of TF1 concentration on the steady-state FPA of ethidium bound to SPO1 DNA [22 μM (bp) DNA and 0.2 μM ethidium in 50 mM NaCl, 10 mM Tris-HCl, and 2 mM Na_2EDTA at pH 7]. The FPA is plotted against the TF1 concentration (insert) and against the TF1/DNA binding ratio, where the concentration of bound protein is obtained from previously described fluorescence titrations (Härd et al., 1989b). Error bars represent estimated standard deviations, and circles represent FPA values corrected for contributions from free dye, as explained in the text. (B) Effect of TF1 concentration on the ethidium fluorescence intensity. [The data in (A) and (B) refer to the same titration.]

density up to $\nu \approx 0.02$ and is thereafter only weakly dependent on the binding density. A similar behavior can be observed for the total fluorescence intensity, which decreases with the TF1 binding density for $\nu < 0.02$ and is independent of ν at $\nu > 0.02$. A decrease in fluorescence intensity indicates a larger fraction of free dye, i.e., a lower ethidium binding affinity in the presence of bound TF1. It is interesting to note that the FPA increase and fluorescence intensity decrease are "correlated" in the sense that both are almost independent of the TF1 binding density at $\nu > 0.02$.

The steady-state FPA is more sensitive to the fraction of free dye than is the time-resolved FPA decay. In our case, where the fraction of free dye is larger in the presence of bound TF1, this effect leads to an underestimate of the FPA of bound ethidium at high binding densities, compared to the corresponding error in the FPA in the absence of bound TF1. The data in Figure 3A were corrected for this effect, by assuming that the ethidium binding constant is (approximately) 10^6 M^{-1} in the absence of TF1 (Waring, 1965), and assuming that the fraction of free dye in the presence of TF1 can be calculated from the fluorescence intensity, as described elsewhere (Härd et al., 1988). It is evident from Figure 3A that these corrections are of little importance to the qualitative behavior of

the steady-state FPA as a function of the TF1 binding density.

Discussion

We have used the time-resolved and steady-state fluorescence polarization of intercalated ethidium to examine the flexibility of SPO1 DNA with and without bound TF1. In the absence of TF1 we find that the fitted measured rigidity of hmUra-containing SPO1 DNA is the same as in other, naturally occurring, T-containing DNAs. The results suggest that any structural differences between T- and hmUra-containing DNAs do not manifest themselves in the dynamics on a nanosecond time scale and that the torsional flexibility of SPO1 DNA is uniform over several hundred base pairs.

We find that the binding of the TF1 protein to SPO1 DNA reduces the ethidium binding affinity and also results in a substantial decrease in the apparent DNA flexibility. The effect is observable at low concentrations of bound TF1 (<1 TF1 dimer/500 DNA bp), corresponding to less than 300 TF1 dimers per SPO1 DNA molecule (145 kbp). The results further suggest that, for binding densities >1 TF1 dimer/50 DNA bp, the TF1 causes no additional change in the mobility or binding of the intercalated dye. The measured DNA torsional rigidity at high TF1 binding densities appears to be about 7 times larger than in the absence of TF1. In fact, the time-resolved FPA decays only moderately within 50 ns at high TF1 binding densities, a behavior that is reminiscent of that observed in chromatin fibers (Ashikawa et al., 1983). We also note that the flexibility at high TF1 binding densities, though restricted, still can be fitted to a model that is derived for a continuous DNA filament, i.e., a model that does not allow for any "singularities" in the form of joints or sharp kinks.

An increase in the FPA of intercalated ethidium can obviously be attributed to a TF1-induced reduction of the DNA torsional flexibility, but other possible explanations should not be ruled out without consideration. For instance, TF1 might instead induce a change in the (local) ethidium binding site geometry, resulting in an apparent decrease in the molecular flexibility. This could arise because the anisotropic nature of DNA torsional motions causes the FPA to be very sensitive to the dye binding site geometry, as discussed in our earlier work (Härd & Kearns, 1986; Härd, 1987) (see also eq 8). However, the observed fluorescence lifetime of bound ethidium, as well as the dye wobbling motions (reflected in the ARF), does not change at high TF1 binding densities (Table I), and this argues against a structural change in the DNA–ethidium complex.

A more trivial explanation of the FPA increase is that the addition of TF1 causes SPO1 DNA to form macroscopic aggregates in which internal DNA motions are suppressed. The effect of TF1 would in this case be similar to the effect of polyamines that are known to condense and precipitate DNA (Gosule & Schellman, 1978). However, we do not consider this mechanism likely, for two reasons. First, we observe the described effects at relatively low DNA concentrations (22 μM DNA bp), where intermolecular aggregation should be disfavored. Second, we are unable to observe any static light scattering indicating aggregation even at the highest TF1 and DNA concentrations used in this study. These arguments suggest that an altered ethidium binding site geometry and/or intermolecular aggregation are not likely to be the cause of the observed FPA increase and that the explanation therefore is a more restricted internal DNA flexibility in the DNA–TF1 complexes.

A reduction of the DNA torsional mobility upon TF1 binding might be due to one of the following mechanisms, or to a combination of them:

(*i*) *Introduction of "Stiff" Regions in the DNA.* It seems reasonable that TF1 binding would affect the internal DNA dynamics within the DNA sequence that is directly involved in the binding. On the basis of previous determinations of the TF1 binding site density at the buffer conditions used here (Härd et al., 1989b) and molecular modeling on a graphics screen (V. Hsu, personal communication), one can estimate that one TF1 dimer might affect the internal DNA dynamics within a sequence of less than 20 bp. According to the elastic model of DNA motions, stiff DNA regions are expected to affect the average torsional flexibility if the lengths of these regions are comparable to the wavelength of the predominant torsional modes ($\approx$100 bp) (Millar et al., 1982). Considering these numbers and that we observe an enhanced FPA at an average binding density of <1 TF1 dimer/500 DNA bp, it seems unlikely that stiff regions in an otherwise straight DNA could account for the observed effect, unless TF1 binding induces long-range structural changes in the DNA. This notion is also supported by a simple model calculation of the effects of enhanced regions of stiffness that are widely spaced within an otherwise "normal" DNA using the expression for the net torsional rigidity of heterogeneous elastic filament devised by Hogan and Austin (1987) (their eq 7). If one assumes that one TF1 dimer binds to 10 DNA base pairs and that the torsional rigidity ($\alpha\gamma$ in eq 7) within this region is 7 times larger than the normal value, as measured at high TF1 binding densities, then the expected increase in the net torsional rigidity constant at low binding densities (<1 TF1 dimer/500 base pairs) is less than 2%! Such a small increase in the net torsional rigidity cannot account for the increase in steady-state FPA observed in Figure 3A (Fujimoto & Schurr, 1986).

(*ii*) *Large Viscous "Drag" Effects Due to the Presence of Bound TF1.* Such effects seem unlikely to affect the FPA at low TF1 binding ratios for the same reasons. (This is beacuse a small change in the friction factor, γ, has the same effect on the observed FPA decay as a small change in the torsional rigidity constant, α, as evident from eq 7.)

(*iii*) *Binding of Ethidium to Sites within or Close to a TF1 Binding Site.* If the dye has a higher affinity for DNA sequences within, or in the vicinity of, initial TF1 binding sites, then the observed FPA would no longer reflect the average dynamic properties of the DNA. If this were true, we might expect to observe an enhanced ethidium binding, whereas the opposite is observed. We note that the high-affinity sites for ethidium binding to chromatin fibers are located within "linker" DNA regions, i.e., DNA sequences that are not covered with protein (Angerer & Moudrianakis, 1972; Kubista et al., 1985). If the binding of TF1 did not affect remote sides on the DNA, it would be difficult to see how low levels of TF1 could displace the ethidium.

(*iv*) *Introduction of "Bent" Regions in the SPO1 DNA.* DNA "bends" or "kinks" are expected to have a larger effect on the FPA than stiff regions in an otherwise (on the average) straight DNA. This is because a "bend" can be expected to disrupt the long-range DNA torsional motions predicted in the elastic DNA model, in a manner similar to the effect of "clamped ends" (Schurr & Schurr, 1985). On the other hand, it is evident that the intermediate zone approximation [eq 4 and 5 (Allison & Schurr, 1979; Schurr, 1984)] for the time-resolved FPA decay still seems to be valid for TF1–SPO1 complexes at high binding densities (Figure 1, Table I), and this would not be the case if (nanosecond) torsional motions could not be sensed "across" sites of bound proteins located at an average distance of 20 bp from each other (Schurr & Schurr, 1985). Thus, it would seem that the observed effect

at low TF1 binding densities, which suggests DNA bending, and the good fit of eq 7 at high binding densities, which indicate that the DNA still behaves as an elastic continuum, together imply that the DNA is forming a continuously bent superstructure, perhaps in the shape of a toroid or a superhelix. A TF1-induced intramolecular condensation/compaction of SPO1 DNA into a chromatin-like structure would be consistent with the observed behavior of the structurally similar HU protein (Rouviere-Yaniv et al., 1979). Intramolecular condensation might also provide an explanation to the apparent "saturation" of the observed effects at binding ratios >1 TF1 dimer/50 DNA bp, because this binding ratio might reflect the minimum number of bound TF1 dimers needed to stabilize the condensed DNA.

Regarding the displacement of bound ethidium, it is interesting to note that the ethidium binding affinity is expected to depend on the DNA torsional flexibility and that this effect provides an explanation as to why the decreases in ethidium binding and DNA flexibility seem to be correlated (Figure 3). The work required to unwind DNA to form a site for ethidium intercalation can be expected to be proportional to the torsional rigidity constant (Landau & Lifshitz, 1986), and this work enters as a positive enthalpy term in the thermodynamic expression for the ethidium binding constant. One can therefore expect ethidium binding to torsionally constrained DNA to be weakened, and this effect has been observed for binding to supercoiled plasmids (Bauer & Vinograd, 1968, 1970) and for ethidium binding to chromatin fibers at various stages of intramolecular compaction (Härd et al., 1988); in addition, analogous effects have been observed for the binding of the phage 434 repressor protein (Hogan & Austin, 1987).

In summary, we find that TF1 binding results in an enhanced FPA of intercalated ethidium, and we argue that this effect is due to a reduction of the average DNA torsional flexibility. We discuss several mechanisms by which TF1 might cause torsional motions in DNA to become more restricted, including the introduction of stiff regions in DNA, viscous effects, ethidium binding in the vicinity of TF1 binding sites, TF1-induced DNA bending, and intramolecular DNA compaction at high TF1 binding densities. On the basis of the arguments given above, we favor a combination of the two latter mechanisms, by which TF1 binding introduces local DNA bending at low binding densities, followed by a more extensive intramolecular compaction of DNA at high binding densities. This interpretation supports the notion that one of the biological functions of TF1 might be to bend the DNA at specific sites.

Acknowledgments

We thank Michael Sayre and Prof. E. Peter Geiduschek for the DNA and protein with which these experiments were performed and for valuable discussions. We acknowledge Victor Hsu for molecular modeling of TF1 binding and Prof. Doug Magde for assistance with time-resolved fluorescence measurements.

References

Allison, S. A., & Schurr, J. M. (1979) *Chem. Phys. 41*, 35–59.
Angerer, L. M., & Moudrianakis, E. N. (1972) *J. Mol. Biol. 63*, 505–521.
Ashikawa, I., Kinosita, K., Jr., Ikegami, A., Nishimura, Y., Tsuboi, M., Watanabe, K., Iso, K., & Nakano, T. (1983) *Biochemistry 22*, 6018–6026.
Barkley, M. D., & Zimm, B. H. (1979) *J. Chem. Phys. 70*, 2991–3007.
Bauer, W., & Vinograd, J. (1968) *J. Mol. Biol. 33*, 141.
Bauer, W., & Vinograd, J. (1970) *J. Mol. Biol. 47*, 419–435.
Drlica, K., & Rouviere-Yaniv, J. (1987) *Microbiol. Rev. 51*, 301–319.
Elias, J. G., & Eden, D. (1981) *Macromolecules 14*, 410–419.
Fujimoto, B. S., & Schurr, J. M. (1986) *J. Phys. Chem 91*, 1947–1951.
Gosule, L. C., & Schellman, J. A. (1978) *J. Mol. Biol. 121*, 311–326.
Greene, J. R., & Geiduschek, E. P. (1985a) *EMBO J. 4*, 1345–1349.
Greene, J. R., & Geiduschek, E. P. (1985b) in *Sequence Specificity in Transcription and Translation* (Gold, L., & Calendar, R., Eds.) pp 255–269, A. R. Liss, Inc., New York.
Greene, J. R., Brennnan, S. M., Andrew, D. J., Thompson, C. C., Richards, S. H., Heinrikson, R. L., & Geiduschek, E. P. (1984) *Proc. Natl. Acad. Sci. U.S.A. 81*, 7031–7035.
Hagerman, P. J. (1981) *Biopolymers 20*, 1503–1535.
Härd, T., Nielsen, P., & Nordén, B. (1988) *Eur. Biophys. J. 16*, 231–241.
Härd, T. (1987) *Biopolymers 26*, 613–618.
Härd, T., & Kearns, D. R. (1986) *J. Phys. Chem. 90*, 3437–3444.
Härd, T., Fan, P., Magde, D., & Kearns, D. R. (1989a) *J. Phys. Chem. 93*, 4338–4345.
Härd, T., Hsu, V., Sayre, M. H., Geiduschek, E. P., Appelt, K., & Kearns, D. R. (1989b) *Biochemistry 28*, 396–406.
Hogan, M., Dattagupta, N., & Crothers, D. M. (1979) *Biochemistry 18*, 280–288.
Hogan, M. E., & Austin, R. H. (1987) *Nature 329*, 263–266.
Johnson, G. G., & Geiduschek, E. P. (1972) *J. Biol. Chem. 242*, 3571–3578.
Kubista, M., Härd, T., Nielsen, P. E., & Nordén, B. (1985) *Biochemistry 24*, 6336–6342.
Landau, L. D., & Lifshitz, E. M. (1986) in *Theory of Elasticity*, Course of Theoretical Physics, Vol 7, 3rd ed., Pergamon Press, Oxford, England.
Magde, D., Zappala, M., Knox, W. H., & Nordlund, T. M. (1983), *J. Phys. Chem. 87*, 3286–3288.
Millar, D. P., Robbins, R. J., & Zewail, A. H. (1982) *J. Chem. Phys. 76*, 2080–2094.
Millar, D. P., Ho, K. M., & Aroney, M. J. (1988) *Biochemistry 27*, 8599–8606.
O'Connor, D. V., & Phillips, D. (1984) in *Time-Correlated Single Photon Counting*, pp 180–189, Academic Press, Orlando, Fl.
Press, W. H., Flannery, B. P., Teukolsky, S. A., & Vetterling, W. T. (1986) in *Numerical Recipes*, Chapter 14, Cambridge University Press, Cambridge, England.
Robertson, C. A., & Nash, H. A. (1988) *J. Biol. Chem. 263*, 3554–3557.
Rouviere-Yaniv, J., Yaniv, M., & Germond, J.-E. (1979) *Cell 17*, 265–274.
Schurr, J. M. (1984) *Chem. Phys. 84*, 71–96.
Schurr, J. M., & Schurr, R. L. (1985) *Biopolymers 24*, 1931–1940.
Shibata, J. H., Fujimoto, B. S., & Schurr, J. M. (1985) *Biopolymers 24*, 1909–1930.
Skibsted, L. H., Hancock, M. P., Magde, D., & Sexton, D. A. (1987) *Inorg. Chem. 26*, 1708–1712.
Stenzel, T. T., Patel, P., & Bastia, D. (1987) *Cell 49*, 709–717.
Tanaka, I., Appelt, K., Dijk, J., White, S. W., & Wilson, K. S. (1984) *Nature 310*, 376–381.
Thomas, J. C., & Schurr, J. M. (1983) *Biochemistry 22*, 6194–6198.
Thomas, J. C., Allison, S. A., Appelof, C. J., & Schurr, J. M. (1980) *Biophys. Chem. 12*, 177–188.

Wahl, P. (1979) *Biophys. Chem. 10*, 91–104.
Wahl, P., Paoletti, J., & Le Pecq, J. B. (1970) *Proc. Natl. Acad. Sci. U.S.A. 65*, 417–421.
Waring, M. J. (1965) *J. Mol. Biol. 13*, 269–282.
Wilson, D. L., & Geiduschek, E. P. (1969) *Proc. Natl. Acad. Sci. U.S.A. 62*, 514–520.
Wu, P., Fujimoto, B. S., & Schurr, J. M. (1987) *Biopolymers 26*, 1463–1488

Spectropolarimetric Analysis of the Core Histone Octamer and Its Subunits†

Jamie E. Godfrey, Andreas D. Baxevanis, and Evangelos N. Moudrianakis*
Department of Biology, The Johns Hopkins University, Baltimore, Maryland 21218
Received May 15, 1989; Revised Manuscript Received September 5, 1989

ABSTRACT: The secondary structure of the calf thymus core histone octamer, $(H2A–H2B–H3–H4)_2$, and its two physiological subunits, the H2A–H2B dimer and $(H3–H4)_2$ tetramer, was analyzed by ORD spectropolarimetry as a function of temperature and solvent ionic strength within the ranges of these experimental parameters where assembly of the core histone octamer exhibits pronounced sensitivity. While the secondary structure of the dimer is relatively stable from 0.1 to 2.0 M NaCl, the secondary structure of the tetramer exhibits complex changes over this range of NaCl concentrations. Both complexes exhibit only modest responses to temperature changes. ORD spectra of very high and very low concentrations of stoichiometric mixtures of the core histones revealed no evidence of changes in the ordered structure of the histones as a result of the octamer assembly process at NaCl concentrations above 0.67 M, nor were time-dependent changes detected in the secondary structure of tetramer dissolved in low ionic strength solvent. The secondary structure of the chicken erythrocyte octamer dissolved in high concentrations of ammonium sulfate, including those of our crystallization conditions, was found to be essentially unchanged from that in 2 M NaCl when examined by both ORD and CD spectropolarimetry. The two well-defined cleaved products of the H2A–H2B dimer, cH2A–H2B and cH2A–cH2B, exhibited reduced amounts of ordered structure; in the case of the doubly cleaved moiety cH2A–cH2B, the reductions were so pronounced as to suggest marked structural rearrangements.

Because of their central role in the compaction and organization of eukaryotic chromosomes, the inner or core histones (H2A, H2B, H3, and H4) have been the objects of structural studies for many years. [For a review of histone and nucleosome structure, see McGhee and Felsenfeld (1980).] The early work of Isenberg, Kelly, and others established that histones H2A and H2B exist as a stable dimeric complex over a broad range of solvent conditions; likewise, histones H3 and H4 have been shown to form the stable tetrameric complex $(H3–H4)_2$ (D'Anna & Isenberg, 1974a,b; Kornberg & Thomas, 1974; Rubin & Moudrianakis, 1975; Roark et al., 1974, 1976; Moss et al., 1976a,b). Although it has been recognized for over 15 years that two each of the inner histones comprise the octameric core of the nucleosomes (Kornberg, 1974; Noll, 1974; Olins et al., 1976), several years elapsed before evidence was presented demonstrating octamer assembly from the stable dimer and tetramer complexes (Eickbush & Moudrianakis, 1978; Ruiz-Carillo & Jorcano, 1979; Jackson & Chalkley, 1981; Worcel et al., 1978; Earnshaw et al., 1982).

From sedimentation equilibrium studies, Godfrey et al. (1980) have shown that core histone octamer assembly in 2 M NaCl can be described by a two-step reversible process involving the two subunits and a hexamer intermediate:

$$H2A–H2B + (H3–H4)_2 \rightleftharpoons H2A–H2B–(H3–H4)_2$$

$$H2A–H2B + H2A–H2B–(H3–H4)_2 \rightleftharpoons (H2A–H2B–H3–H4)_2$$

Eickbush and Moudrianakis (1978) explored the temperature and solvent ionic strength dependencies of the core histone assembly system by gel filtration. These studies revealed that the subunit interactions which are strong in 2 and 4 M NaCl decrease markedly at lower salt concentrations. The temperature sensitivity of the system was also found to be unusually pronounced.

The question arises as to whether changes, if any, which can be detected in the secondary structure of the core octamer subunits as a function of temperature and solvent ionic strength correlate well with the sensitivity of the octamer assembly process to these experimental parameters. It is also of interest to know whether the assembly process itself is accompanied by any alteration in the secondary structure of the histones. A number of spectropolarimetric studies on the secondary structure of histones have been reported since the early work of Isenberg and his co-workers (D'Anna & Isenberg, 1974a–c; Moss et al., 1976a,b; Beaudette et al., 1981; Prevelige & Fasman, 1987; Park & Fasman, 1987; and references cited therein). These studies have examined histones under a variety of solvent conditions; however, none have attempted a *systematic survey* of the core histone octamer or its physiological subunits over the temperature and solvent ionic strength ranges

† Publication No. 1446 from the Department of Biology, The Johns Hopkins University. This research was supported in part by a grant from the National Institutes of Health (GM33495 to E.N.M.).
* To whom correspondence should be addressed.

0006-2960/90/0429-965$02.50/0